Journal of the European Ceramic Society 21 (2001) 2243–2251

www.elsevier.com/locate/jeurceramsoc

# Creep damage in different $3Al_2O_3{\cdot}2SiO_2$ mullites tested in 4-point bending

E. Fernandez, C. Baudín *

*Instituto de Cerámica y Vidrio, 28 500 Arganda del Rey Madrid, Spain*

Received 7 September 2000; received in revised form 22 November 2000; accepted 9 December 2000

**Abstract**

The creep behaviour in 4-point bending at 1200°C of two nominally $3Al_2O_32SiO_2$ materials and that of other materials prepared by annealing one of these two materials at the sintering temperature as well as at 900 and 1200°C have been studied. All materials presented very little or no glassy phase at the grain boundaries. Special preparation of the samples for microstructural analysis by scanning electron microscopy has been used in order to characterise the "as crept" parts of the samples subjected to tension as well as compression during the creep experiments. In all materials highly vitrified dense zones have been observed close to the tension and compression surfaces. Viscous cavity growth has been detected at depths (≈20–50 μm) from the tension and compression surfaces that vary from one material to the other and increase with the applied stress. Strain values for all materials are very low and do not reflect the extreme microstructural modifications observed in the samples. Densification and cavity growth can be explained on the basis of the viscous cavity growth model. Stress-enhanced dissolution of the mullite grains is proposed to be the origin of the large amounts of vitreous phase present in the samples after testing. 

*Keywords:* Creep; Damage; Failure analysis; Mullite

## 1. Introduction

Mullite materials for structural applications have been widely investigated during the last 30 years. In particular, much attention has been paid to creep processes in high purity (>99 wt.%), dense ($\geqslant$ 99%$\rho_{th}$) and fine grained (≈0.5–3 μm) mullites with compositions close to the stoichiometric $3Al_2O_3{\cdot}2SiO_2$, after the first data by Lessing et al.[1] that reported a creep rate in compression lower than that of alumina of the same grain size under the same experimental conditions.

Most creep work has been done in flexure[1–11] as well as in compression.[11–15] Materials with different microstructures and compositions ranging from 67 to 82 wt.% of alumina have been characterised and a wide range of activation energies (Q≈357–1051 kJ/mol), stress exponents ($n$≈0.2–2.7) and grain size exponents ($p$≈1–3.7) have been determined in experiments at stresses from 0.2 to 300 MPa and temperatures from 1100 to 1500°C. In general, grain boundary sliding (GBS) is considered the main deformation mechanism and that the strain rates are controlled by viscous flow of amorphous grain boundary phases, diffusion, solution-precipitation and/or cavitation. It is generally agreed that the broad range of reported creep parameters are due to differences in experimental conditions — loading arrangement, temperature and stress- as well as in microstructure and composition of the studied materials.

In a previous work,[10] the creep behaviour in 3-point bending of four nominally $3Al_2O_3{\cdot}2SiO_2$ stoichiometric mullite materials were studied. Two of them (MB0 and MS0) were fabricated from commercial powders with different impurities (MS[1]: $ZrO_2 = 0.33$ wt.%, $TiO_2 = 0.13$ wt.%, $Na_2O + K_2O + CaO + MgO = 0.13$ wt.%; MB[2]: $Na_2O = 0.18$ wt.%, $Fe_2O_3 = 0.10$ wt.%, $K_2O + CaO + MgO = 0.12$ wt.%) and the other two (MST, MBT) were obtained by annealing of these two materials at the sintering temperatures during 24 h. In spite of differences in composition, microstructure and in the high temperature mechanical behaviour under monotonously increasing loads,[10,16–17] the creep data obtained for the four materials were very similar.

The stress exponents ($2.17 < n < 2.55$), determined by a stress change technique, as well as the apparent activation

* Corresponding author. Fax: +34-91-870-05-50.
*E-mail address:* cbaudin@icv.csic.es (C. Baudín).

[1] Chichibu Cement Co., Japan.
[2] 193CR, Baikowski Chimie, France.

0955-2219/01/$ - see front matter 
PII: S0955-2219(00)00324-1

energies (705 kJ/mol < $Q$ < 742 kJ/mol), determined by successive temperature jumps in the 1200–1400°C range, were very close for all the materials and in the range of those reported for densification of hot pressed mullite. On the basis of the similarities that exist between creep and densification, a solution-diffusion through liquid phase-precipitation mechanism with interface reaction being the rate controlling step was proposed for creep.

For a material made of the same powder as MB0 and similar microstructure, long term experiments in 4-point bending at temperatures between 1200 and 1400°C lead to lower values of the stress exponent ($n \approx 1$) and higher activation energy (≈860 kJ/mol), as reported by other authors.[6] No significant cavitation was observed on polished and etched tensile surfaces of samples tested at 1200°C.

For a material prepared from the same MS0 powder[5] tested in 4-point bending using the incremental stress method in the temperature range 1365–1460°C, a dependence of stress exponent on temperature ($n = 1.02$ at 1365°C, $n = 1.52$ at 1480°C) and stress ($n = 1.19$ for $\sigma \leqslant 50$ MPa, $n = 1.95$ for $\sigma > 50$ MPa, at 1460°C) and high activation energies (860–880 kJ/mol) were reported. No significant cavitation was observed on polished and etched tensile surfaces of creep fractured samples tested at 1460°C in the low stress range (< 100 MPa).

Differences between creep data reported by other authors[5,6] and our previous data might be due to differences in experimental conditions leading to different microstructural evolutions of the materials during the creep experiments. In particular, annealing experiments without loading have revealed that MB0 experiences significant microstructural changes after 48 h at 1200°C,[18] which might imply that a real stationary creep state is not attained during creep experiments.

In this work, a careful analysis of the microstructure of tested samples has been performed in order to understand the creep behaviour in bending of MB0 and MS0 mullites. These two base materials as well as other materials prepared by annealing MB0 have been studied. In principle, creep damage could be expected to occur in the areas in tension as well as in compression of bending samples. Moreover, preparation of the tension surfaces for microstructural analysis by polishing and etching might imply the removal of some of the damaged area close to the parts of the samples subjected to the maximum stresses. A special preparation of the samples for microstructural analysis has been used in order to assure the complete characterisation of the microstructural changes experienced by the samples.

## 2. Experimental

The two base materials, MS0 and MB0, discussed previously and additional materials prepared by annealing MB0 at different temperatures (MB900:900°C, MB1200: 1200°C, MB1630: 1630°C = sintering temperature) have been studied. The fabrication method as well as the microstructural characterisation of all the materials have been reported elsewhere.[16–18] Average grain sizes of the MB materials range from 1.3 μm for MB1630 to 0.6 μm for MB1200 and for MS0 average grain size is 1.2 μm. Materials MB1200, MB1630 and MS0 present a bimodal microstructure made of a mixture of equidimensional and tabular grains. Remaining glass is mostly located at triple points in MB0, MB900 and MS0, forming small (< 250 nm) pockets, whereas thin films (< 50 nm) are found across grain boundaries in MB1200 and MB1630.

The starting powders differentiate not only in the impurity contents but also in the alumina/silica molar ratio, which is slightly higher for MB (1.62)[11,16] than for MS (1.57).[16]

In order to determine the lattice parameters of mullite in the MB materials, X-ray diffraction studies were carried out with a computer-controlled powder diffractometer

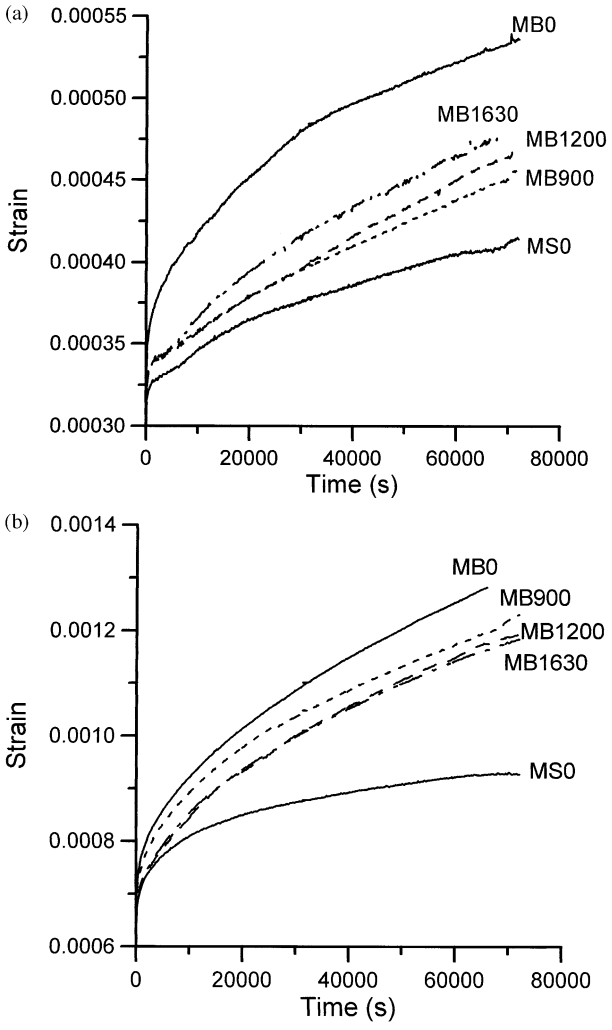


Fig. 1. characteristic strain-time plots for all the materials. (a) load = 69 N; (b) load = 138 N.

(D5000, Siemens, Germany) using Ni-filtered Cu$K_{\alpha 1}$ radiation. Diffraction patterns were recorded in the 36–65° 2θ range, in the step scan mode (6 s, 0.03°, 2θ) with Si as internal standard, and a computer program for lattice parameter refinements (Fargo 58105-5516, North Dakota State University, USA) was used for calculations.

For creep tests, bars ($3\times4\times50$ mm$^3$) were diamond machined from the sintered blocks and chamfered. The surface to be in tension during the bending experiments was polished with diamond down to 3 μm.

Creep tests were performed at 1200°C, in an universal load testing machine with an electrically heated furnace (INSTRON 6000, Great Britain) using 4-point bending fixtures made of alumina with inner and outer spans of 20 and 40 mm. Two levels of static load (69, 138 N), which correspond to the stress level used by other authors for MB0[6] and MS0[5] (≈58, 115 MPa) during 20 h were applied. The central point deflection of the bars was measured using a SiC probe attached to a linear voltage displacement transducer through an alumina tube. Stress and strain were calculated by the procedure given by Hollenberg et al.[19] assuming a stress exponent of unity. No further corrections to the estimated stresses and strains were made.

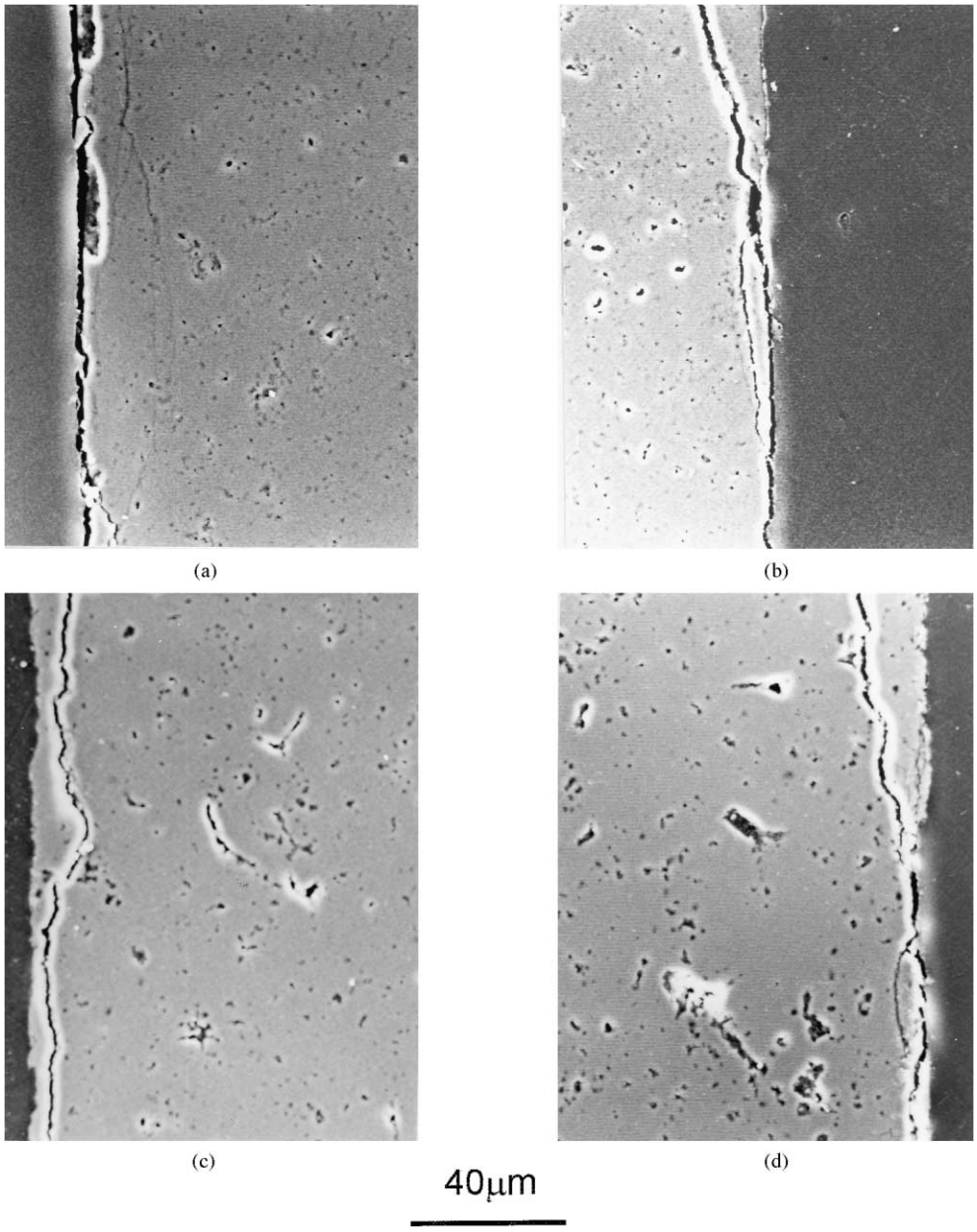


Fig. 2. SEM micrographs of the lateral surfaces of the central parts of samples tested at 69 N. Diamond polished and unetched surfaces. (a) MB0: the tension surface is located at the left end of the sample; (b) MB0; the compression surface is located at the right end of the sample; (c) MS0: the tension surface is located at the left end of the sample; (d) MS0: the compression surface is located at the right end of the sample.

For microstructural observations after testing, the central parts of the samples were cut and lateral surfaces, perpendicular to the tension and compression surfaces, across the length of the samples were diamond polished down to 1 μm. These samples were allowed to characterise the tension as well as the compression areas of the bars from the outer surfaces to the centre of the sample. As polished surfaces were observed. Additional observations were performed on the tension surfaces of the crept samples after polishing and thermally etching (1500–30 min). All microstructural characterisation was done by scanning electron microscopy (SEM-EDX, Carl Zeiss DSM-950, Germany).

## 3. Results

In spite of slight variations from one material to the other, the lattice parameters of mullite in the four MB materials could be included in a range ($a = 7.543 \pm 0.002$, $b = 7.682 \pm 0.002$, $c = 2.8823 \pm 0.0002$ Å) corresponding to a stoichiometric $3Al_2O_3 2SiO_2$ mullite, as determined by other authors for MS0[5] ($a = 7.5466$, $b = 7.6932$, $c = 2.8847$ Å).

Fig. 1 shows characteristic strain-time plots for all the materials. Strains of the MB materials are larger (≈20–50%) than those of MS0 at both stress levels and those of MB0 are always larger than those of the annealed materials. The extent of strain is very similar for the three annealed materials and it is intermediate between those of MB0 and MS0.

Low magnification micrographs of polished and unetched tested samples are shown in Figs. 2–4. In all samples highly damaged zones, constituted of dense areas separated from the rest of the sample by large cracks, were found close to the tension and compression surfaces. The tension surfaces, which were polished before the creep tests, presented highly irregular topographies, even with voids (Fig. 2a). This aspect seems to be due to the separation of the dense areas surrounded by cracks, as those observed in Fig. 2b–d, during cooling from the testing temperature.

For each material, the sizes of the damaged zones close to the tension and compression surfaces were similar for the same applied stress (Fig. 2a and b and Fig. 2 c and d), and were larger when higher stresses were applied (Figs. 2–3a, Fig. 2c and Fig. 3b). For the same applied stresses, these damaged zones in the MB-annealed materials were smaller than those in MB0 (2a, 4a–b, 3a, 4c). In the interior of the specimens, cavities as well as apparently undamaged zones were randomly distributed across the whole section of the specimens (Figs. 2–4). In MS0, a lower number of larger cavities (up to 20 μm) than in the MB materials, in which smaller ($< 10$ μm) cavities were found, were observed.

Larger magnification micrographs of the cracks revealed highly vitrified zones, with rounded cavities, which appear to be the origins of the cracks (Figs. 5 and 6a). For the same applied stress, the size of the rounded cavities was larger for MB0 (Fig. 5a) than for MS0 (Fig. 5b). For the MB materials (Fig. 5a–e), the size of the cavities decreased with the temperature of annealing but this decrease in size

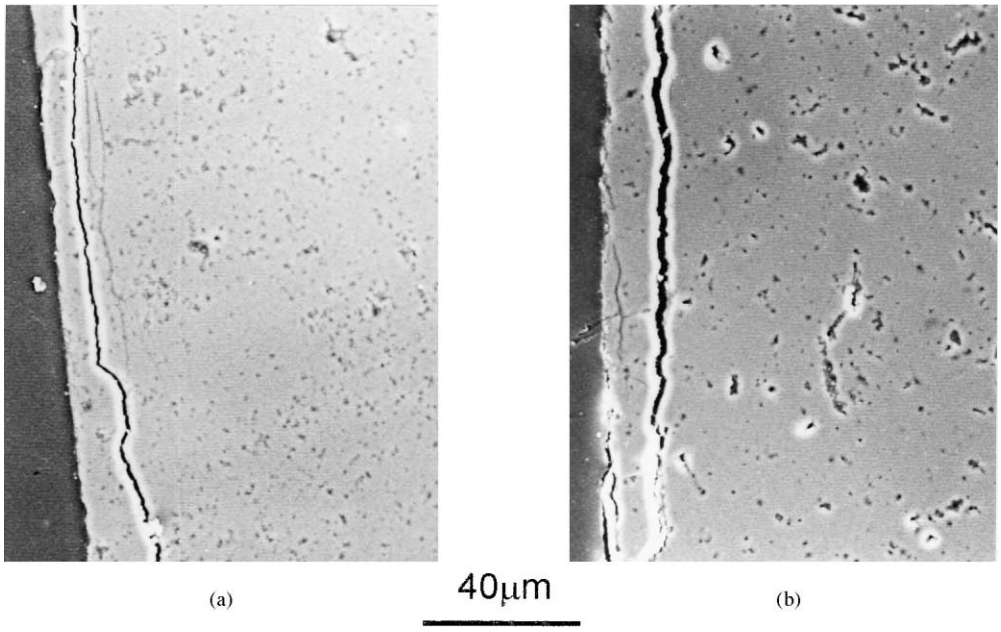


Fig. 3. SEM micrographs of the lateral surfaces of the central parts of samples tested at 138 N. Diamond polished and unetched surfaces. The tension surface is located at the left end of the samples. (a) MB0; (b) MS0.

was linked to an increase in the number of cavities for the same crack length found in MB1200 and MB1630.

As shown in Fig. 6b and c, vitrification was also observed inside the large cavities located close to the tension and compression surfaces.

Semiquantitative analysis (EDX) performed on MB0 unetched crept samples gave low alumina/silica molar ratios (≈1.2–1.3) in the highly vitrified areas inside the cracks such as that shown in Fig. 6a, and no differences were found between the ratios (≈1.69) corresponding to the large cavities (Fig. 6b) and the average ratio for areas (≈4 $\mu m^2$) across a line located at 400 μm from the tension surface (1.75±0.05). These last values are slightly higher than those determined by chemical analysis (1.62) and by EDX on "as fabricated" samples (1.63±0.02).

## 4. Discussion

Two main points are derived from the experimental results described above. First, the extreme microstructural modifications in the crept samples in areas close ( < 50 μm) to the tension and compression surfaces (Figs. 2–4), and second, the high concentrations of vitreous phase found inside the cracks (Figs. 5, 6a) as well as in the cavities (Fig. 6b and c) formed in all materials.

The strains calculated in a classical way from the deflection of the central point of the samples using Hollenberg's equations (Fig. 1) are very low, and in the range of those reported for different mullites. In particular, for MB0 strain-time, relations are practically coincident with those reported for the same material tested at the same

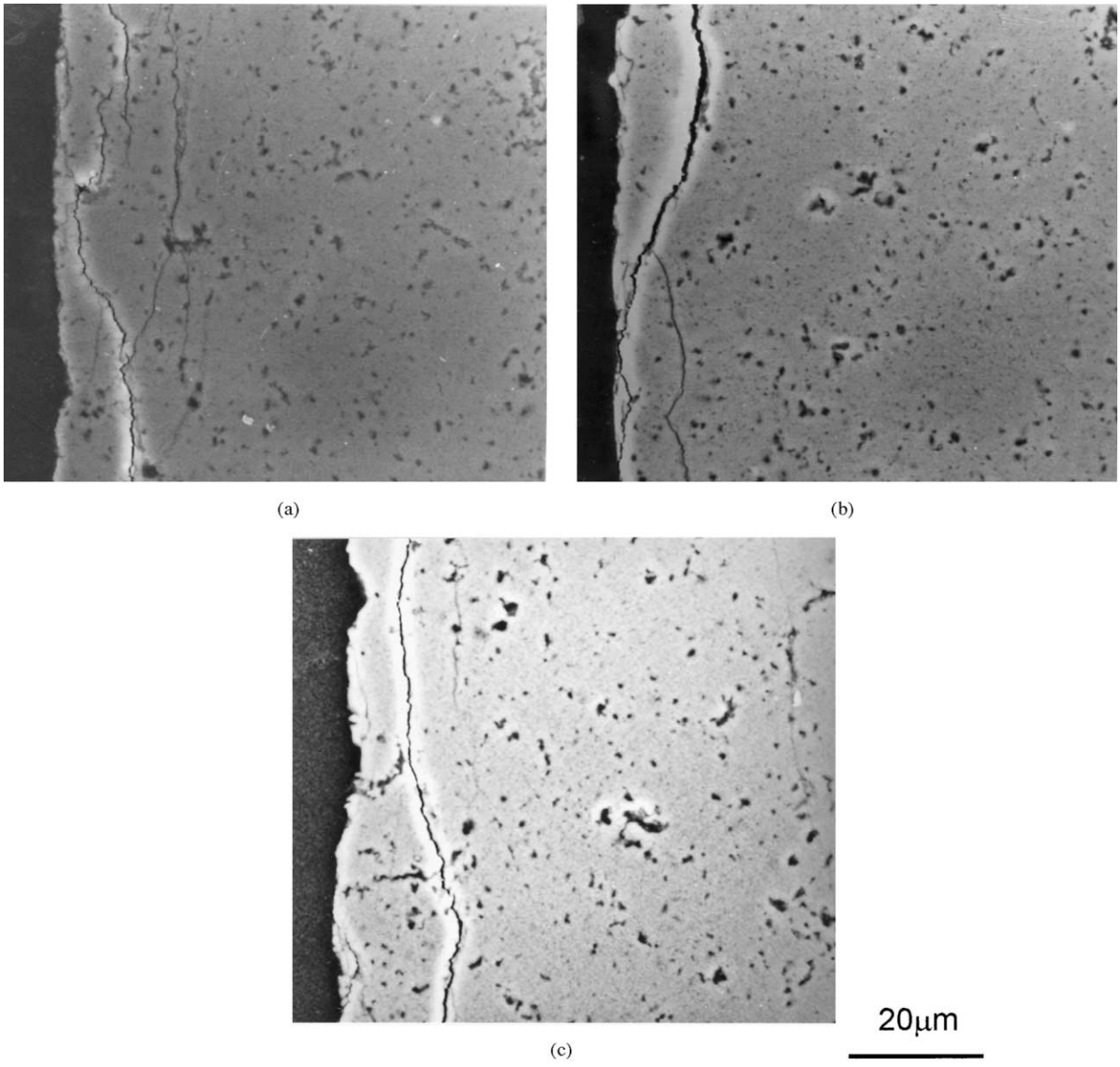


Fig. 4. SEM micrographs of the lateral surfaces of the central parts of tested samples. Diamond polished and unetched surfaces. The tension surface is located at the left end of the samples. (a) MB1630 tested at 69 N; (b) MB1200 tested at 69 N; (c) MB900 tested at 138 N.

temperature and using the same stress range.[6] But, these strain values do not reflect the extreme microstructural modifications close to the tension and compression surfaces. In particular, the large vitrified areas (Figs. 5 and 6a) that for MB0 have been proved to have lower alumina/silica molar ratios than the average in the "as fabricated" material (1.2–1.3 vs 1.63±0.02). In fact, the aspect of the round cavities found inside the large

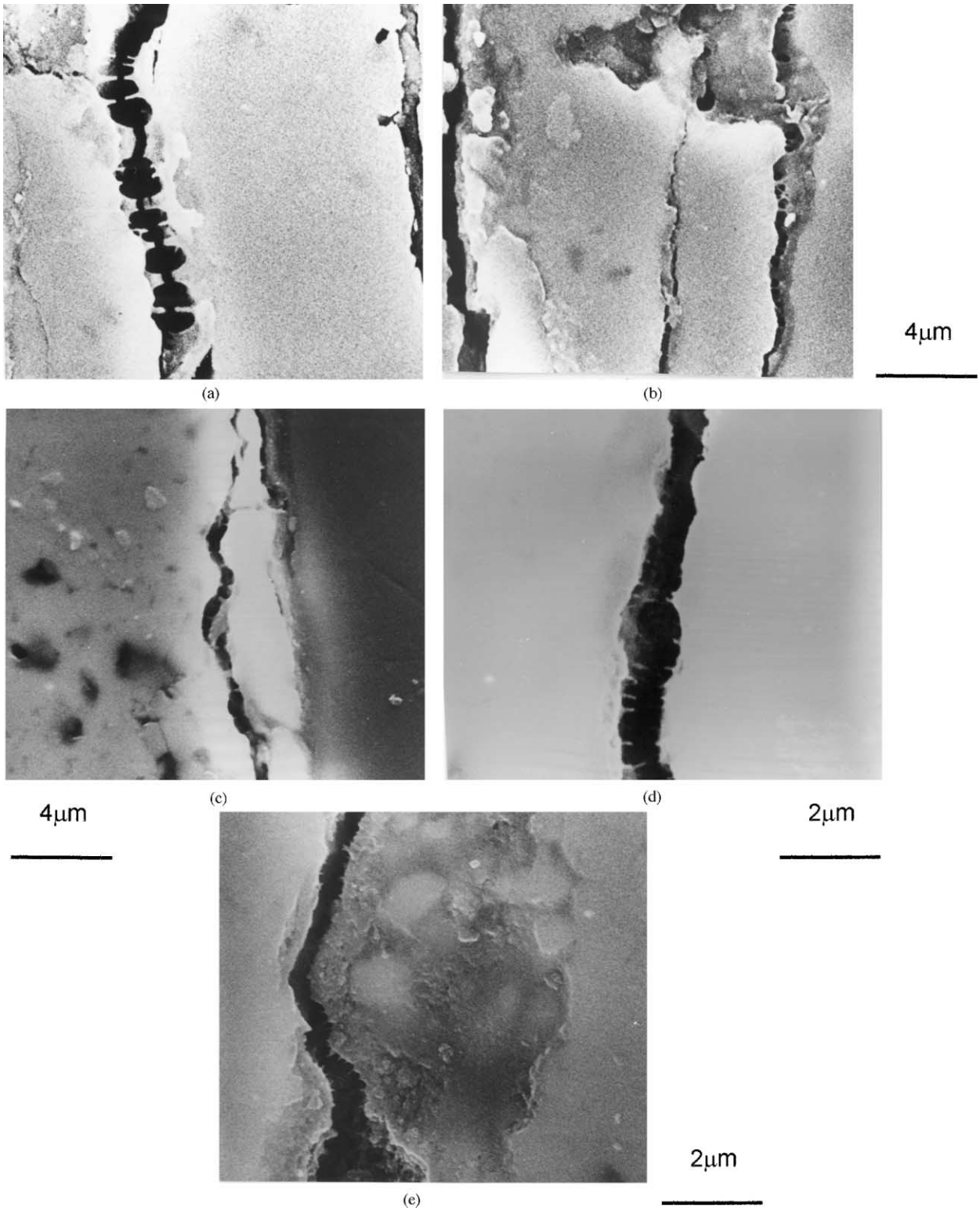


Fig. 5. Internal aspect of the cracks parallel to the tension and compression surfaces shown in Figs. 2 and 3. Highly vitrified zones with rounded cavities are observed. SEM micrographs of diamond polished and unetched surfaces of samples tested at 69 N. (a) MB0; (b) MS0; (c) MB900; (d) MB1200; (e) MB1630.

cracks is the same as that for viscous hole growth within the second phase in ceramics in which grain boundaries are coated with glassy phase.[20] Kinetics of cavity nucleation and growth are dependent on the normal stress acting across the cavitating grain boundary and, therefore, the cavitation process does not depend on whether the local stress at the grain boundary is originated by a remote tensile or compressive stress. Thus, even though identical cavitation kinetics are not necessarily expected in compression and tension, damaged regions are observed close to the tension and compression surfaces of the samples (Fig. 2).

The fact that these viscous growth cavities are found only from a certain distance of the compression and tension surfaces and that dense zones are found between the cracks containing such cavities and the surfaces (Figs. 2–4), might be explained by the viscous cavity growth model that predicts that for:

$$\eta/\varepsilon'\gamma < \text{cavity radius/spacing}$$

($\eta$ = viscosity, $\varepsilon'$ = strain rate, $\gamma$ = surface energy), cavity shrinkage occurs.[20] Considering $\eta$ and $\gamma$ constant for the same material, $\varepsilon'$ will be higher in the zones of the

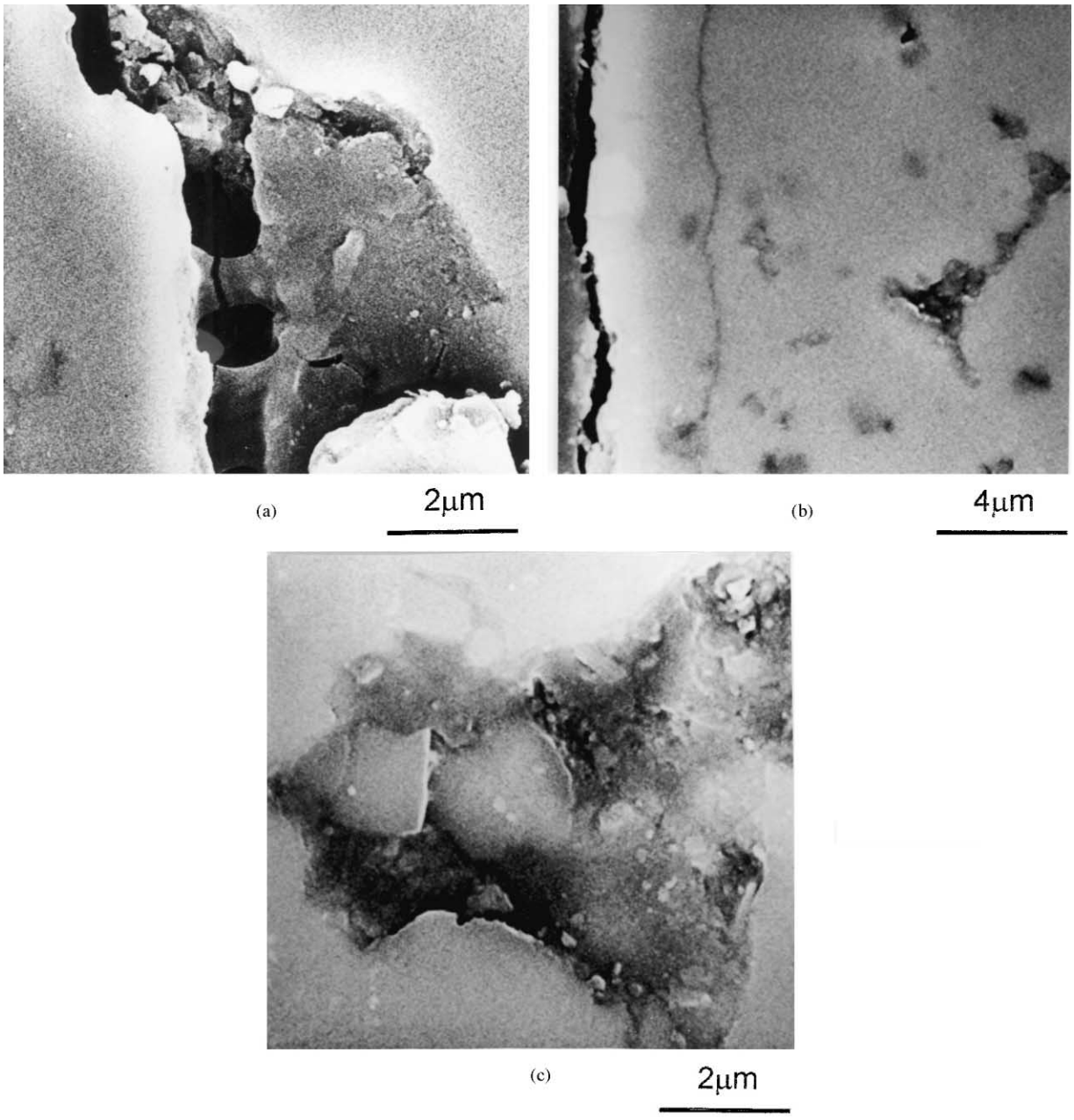


Fig. 6. Internal aspect of the vitrified zones observed in the lateral surfaces of the central parts of tested samples. SEM micrographs of diamond polished and unetched surfaces. (a)MB0 tested at 138N. Cracks parallel to the tension and compression surfaces. (b) MB0 tested at 69 N. Internal cavities. (c) MS0 tested at 138 N. Internal cavities.

sample subjected to maximum stresses (i.e. close to the tension and compression surfaces) and cavity shrinkage in these zones would be more likely to occur than in the bulk of the samples. This viscous densification of the zones close to the tension and compression surfaces would lead to the low apparent strains observed (Fig. 1) as well as to the cracking of the samples during cooling from the creep test temperature (Figs. 2–4). For the same material, higher stresses would imply a larger size of the densification zones and cracks would be located at larger distances from the surfaces, as experimentally observed (Figs. 2a,c and 3).

The most striking result of this work is that large areas of viscous phase creep (Figs. 5–6) have been observed by SEM in materials in which very little amounts of glassy phase were detected, by transmission electron microscopy and located mostly at triple points (MB0, MB900, MS0)[16–18] or as thin films at the grain boundaries (MB1200 and MB1630),[18] before testing. These areas have never been reported to form in the tension surfaces of different mullite materials probably due to the polishing and etching of the surface previous to SEM observations, as the removal of 20–50 μm depth of the sample might occur. As a term of comparison, Fig. 7 shows micrographs of "as fabricated" and the tension surface of crept MB0 samples. Both surfaces have been polished and thermally etched. The aspect of both microstructures is very similar because triangular cavities are present, not only after the creep tests but also in the "as fabricated" material, as pointed out by other authors[6] and shown in Fig. 7.

Ageing studies at 900–1200°C for the mullite containing larger amounts of alkalis, MB0, showed that partial dissolution of the mullite grains occurred and it was attributed to the facts that the lowest invariant points in the system $Al_2O_3$–$SiO_2$–$Na_2O$ are located in this temperature range and that impurities are concentrated at triple points, giving local compositions different from the average composition of the material.[18] Nevertheless, the amounts of liquid phase formed were very little for ageing times up to 48 h. In this work, the formation of highly vitrified areas has been observed even in samples aged at the testing temperature (MB1200, Fig. 5d) and in a low alkali containing mullite (MS0, Figs. 5b and 6c).

The high concentrations of silica found in the vitrified areas close to the tension and compression surfaces indicate that liquids migrate to the highly stressed parts of the samples during testing. Whether these liquids are those originally present in triple points and/or along grain boundaries in the "as fabricated" materials, or have been formed by stress enhanced dissolution of the mullite grains during testing is not completely clear. But, the higher alumina/silica ratios found by EDX inside the cavities and at 400 μm of the tension surfaces of MB0 tested samples (≈1.69, 1.75±0.05), compared to those determined by chemical analysis and EDX for the "as fabricated" material (1.62, 1.63±0.02), support stress enhanced dissolution of the mullite grains. Moreover, large vitrified areas are found in all the samples after testing whereas the remaining glassy phase in the "as fabricated" materials was only detected by transmission electron microscopy.[16,18]

Dissolution of the mullite grains and viscous flow densification at the highly stressed areas of the samples might be responsible for disparity of creep data for

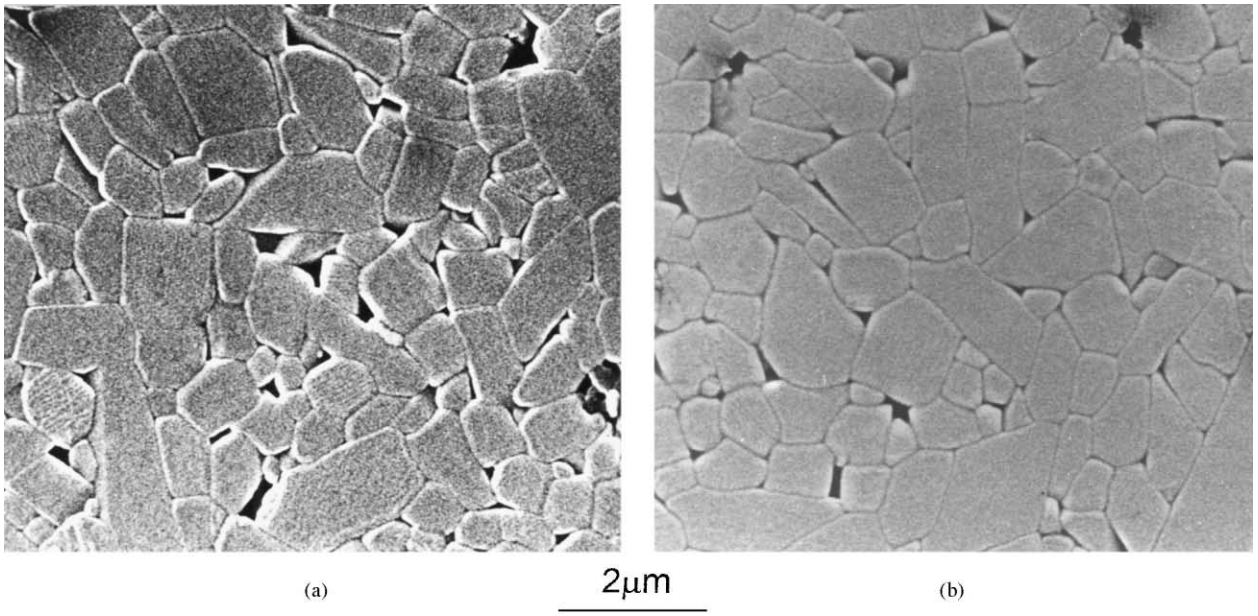


Fig. 7. Comparison between the microstructure of "as fabricated" and tested MB0 samples. The same kind of triangular cavities are observed. SEM micrographs of polished and thermally etched (1500°C–30 min) surfaces. (a) "As fabricated" sample; (b) tension surface of a crept sample tested at 69 N.

stoichiometric mullites ($3Al_2O_3{\cdot}SiO_2$), as only apparent steady creep state would be attained even during long term tests. The high stress coefficients previously obtained for these mullites ($n \geqslant 2.17$) and the values of the activation energies (705–742kJ/mol), close to those obtained for densification of hot pressed mullite,[10] agree with dissolution and densification controlling the measured strains in bending.

## 5. Conclusions

Creep damage in five high purity and dense nominally $3Al_2O_3{\cdot}2SiO_2$ mullite materials with different microstructures and compositions tested in bending has been studied. In all the materials, highly vitrified areas have been observed close to the tension and compression surfaces. Viscous cavity growth has been detected at depths from the tension and compression surfaces, that vary from one material to the other and increase with the applied stress. The large amounts of glass observed in the crept samples as well as analysis of the compositions of different areas of samples of one of the materials indicate that stress enhanced dissolution of the mullite grains occurs during creep tests.

## Acknowledgements

This work was supported by CICYT (Spain), Contract MAT00-0949.

## References

1. Lessing, P. A., Gordon, R. S and Mazniyasni, K. S., Creep of polycrystalline mullite. *J. Am. Ceram. Soc.*, 1975, **58**(3–4), 149.
2. Ashikuza, M., Okuno, T. and Kubota, Y., Creep of mullite materials. *Yogyo Kyokaishi*, 1989, **97**(6), 662–668.
3. Ohnishi, H., Maeda, K., Nakamura, T. and Kawanami, T., High temperature mechanical properties of mullite ceramics. In *Ceram. Trans. Vol. 6, Mullite and Mullite Matrix Composites*, ed. S. Somiya, R. F. Davies and J. A. Pask. The Am. Ceram. Soc. Inc, Westerville, OH, 1990, pp. 605–612.
4. Penty, R. A. and Hasselman, D. P. H., Creep kinethics of high purity, ultra-fine grain polycrystalline mullite. *Mater. Res. Bull*, 1972, **7**(10), 1117–1124.
5. Okamoto, Y., Fukudome, H., Hayashi, K. and Nishikawa, T., Creep deformation of polycrystalline mullite. *J. Eur. Ceram. Soc.*, 1990, **6**(1), 161–168.
6. Torrecillas, R., Comportamiento mecánico de mullita y mullita-circona obtenida por sinterización reactiva. PhD thesis, Universidad Nacional de Educación a Distancia, Madrid, Spain, 1990.
7. Jakus, K. and Wiedehorn, S. M., Creep deformation of ceramics in four-point bending. *J. Am. Ceram. Soc.*, 1988, **71**(10), 832–836.
8. Ashizuka, M., Honda, T. and Kubota, Y., Effects of grain size on creep of mullite ceramics. *J. Ceram. Soc. Jpn. Int. Ed.*, 1991, **99**(4), 282–285.
9. Ohira, H., Ismail, M. G. M. U., Yamamoto, Y., Akiba, T. and Somiya, S., Mechanical properties of high purity mullite at elevated temperatures. *J. Eur. Ceram. Soc.*, 1996, **16**(2), 225–229.
10. Baudín, C., Osendi, M. I., Descamps, P. and Cambier, F., High temperature mechanical properties and creep behaviour of different mullites. In *Key Engineering Materials Vol 132, Euro Ceramics V*, ed. P. Abelard, M. Boussuge, Th. Chartier, G. Lozes, G. Lozes and A. Rousset. Trans. Tech. Publications, Switzerland, 1997, pp. 591–594.
11. Torrecillas, R., Calderón, J. M., Moya, J. S., Reece, M. J., Davies, C. K. L., Olagnon, C. and Fantozzi, G., Suitability of mullite for high temperature applications. *J. Eur. Ceram. Soc.*, 1999, **19**(11), 2519–2527.
12. Dokko, P. C., Pask, J. A. and Mazdiyasni, K. S., High-temperature mechanical properties of mullite under compression. *J. Am. Ceram. Soc.*, 1977, **60**(3–4), 150–155.
13. Nixon, R. D., Chevacharoenkul, S., Davis, R. F. and Tiegs, T. N., Creep of hot-pressed SiC whisker reinforced mullite. In *Ceram. Trans. Vol. 6, Mullite and Mullite Matrix Composites*, ed. S. Somiya, R. F. Davies and J. A. Pask. The Am. Ceram. Soc, Westerville. OH, 1990, pp. 579–603.
14. Calderón-Moreno, J. M. and Torrecillas, R., High temperature creep of polycrystalline mullite. In *Key Engineering Materials Vol 132, Euro Ceramics*, ed. P. Abelard, M. Boussuge, Th. Chartier, G. Lozes, G. Lozes and A. Rousset. Trans Tech. Publications, Switzerland, 1997, pp. 587–590.
15. Hynes, A. P. and Doremus, R. H., High-temperature compresive creep of polycrystalline mullite. *J. Am. Ceram. Soc.*, 1991, **74**(10), 2469–2475.
16. Osendi, M. I. and Baudín, C., Mechanical properties of mullite materials. *J. Eur. Ceram. Soc.*, 1996, **16**(2), 217–224.
17. Baudín, C., Fracture mechanisms in a stoichiometric $3Al_2O_32$-$SiO_2$ mullite. *J. Mater. Sci.*, 1997, **32**(8), 2077–2086.
18. Baudín, C. and Villar, M. P., Influence of thermal aging on microstructural development of mullite containing alkalis. *J. Am. Ceram. Soc.*, 1998, **81**(10), 2741–2745.
19. Holleberg, G. W., Terwillinger, G. R. and Gordon, R. S., Calculation of stresses and strains in four-point bending creep tests. *J. Am. Ceram. Soc.*, 1971, **54**(4), 196–199.
20. Chan, K. S. and Page, A., Creep damage development in structural ceramics. *J. Am. Ceram. Soc.*, 1993, **76**(4), 803–826.